

MmWave Channel Estimation via Atomic Norm Minimization for Multi-User Hybrid Precoding

Junquan Deng*, Olav Tirkkonen* and Christoph Studer†

*Department of Communications and Networking, Aalto University, Finland

†School of Electrical and Computer Engineering, Cornell University, NY, USA

Abstract—To perform multi-user multiple-input and multiple-output transmission in millimeter-wave (mmWave) cellular systems, the high-dimensional channels need to be estimated for designing the multi-user precoder. Conventional grid-based compressed sensing (CS) methods for mmWave channel estimation suffer from the basis mismatch problem, which prevents accurate channel reconstruction and degrades the precoding performance. This paper formulates mmWave channel estimation as an Atomic Norm Minimization (ANM) problem. In contrast to grid-based CS methods which use discrete dictionaries, ANM uses a continuous dictionary for representing the mmWave channel. We consider a continuous dictionary based on sub-sampling in the antenna domain via a small number of radio frequency chains. We show that mmWave channel estimation using ANM can be formulated as a semidefinite programming (SDP) problem, and the user channel can be accurately estimated via off-the-shelf SDP solvers in polynomial time. Simulation results indicate that ANM can achieve much better estimation accuracy compared to grid-based CS, and significantly improves the spectral efficiency provided by multi-user precoding.

I. INTRODUCTION

In future millimeter-wave (mmWave) cellular networks, large antenna arrays are expected to be applied at the base station (BS) to serve multiple user equipments (UE) in dense urban scenarios. To perform multi-user (MU) downlink (DL) hybrid precoding [1], accurate channel state information (CSI) is required. As mmWave channels are likely to be sparse, compressed sensing (CS) methods have been considered for mmWave channel estimation [1]–[5]. In order to apply CS to channel estimation, a discretization procedure is generally adopted to reduce the continuous angular or delay spaces to a finite set of grid points, e.g., using a discrete Fourier transform (DFT) matrix as the dictionary to represent the user channels. Assuming that the direction of departure (DOD) and direction of arrival (DoA) are exactly on the grid, the virtual channel representation is sparse with few non-zero entries. The channel estimation problem then can be addressed with a specific measurement matrix and a recovery algorithm, e.g., the orthogonal matching pursuit (OMP) [2], [5], [6]. However, as the actual signals are continuous and will not fall on the discrete points, power leakage and basis mismatch will degrade recovery performance [7]. Although finer grids can reduce the reconstruction error, they require large amounts of computation resources.

In the literature, most of the MU hybrid precoding schemes assume perfect CSI at the transmitters (see e.g., [8], [9]). However, grid-based CS for channel estimation will lead to the basis mismatch problem and hence channel estimation errors,

which will degrade the performance of MU precoding, such as hybrid precoding with baseband zero-forcing (ZF) [1]. Recently, the continuous basis pursuit with auxiliary interpolation points [10] was used for mmWave channel estimation in [11], which shows that adding interpolation points to the original grids can improve channel estimation accuracy considerably. This paper considers a continuous dictionary for MU mmWave channel estimation in order to completely eliminate the basis mismatch error. More specifically, we proposed using a continuous dictionary based on antenna-domain sub-sampling via a much smaller number of radio frequency (RF) chains in the hybrid mmWave architecture. The sparse mmWave channel estimation then can be formulated as an Atomic Norm Minimization (ANM) problem [12], which can be solved via semidefinite programming (SDP) in polynomial time. ANM has been considered for massive MIMO channel estimation [13], [14], but a fully-digital architecture is assumed which has high complexity compared to hybrid architectures. To show the advantage of ANM based on antenna-domain sub-sampling in the hybrid architecture, we investigate a low-complexity MU hybrid precoding scheme using the estimated channel information. Finally, we evaluate the performance of ANM and the precoding scheme via simulations in realistic scenarios. Simulation results regarding the channel estimation error and user spectral efficiency are provided, which confirm the efficacy of our solutions.

II. SYSTEM MODEL

A. Architectures of BS and UE

We consider a mmWave cellular system where the BS employs N antennas and Q RF chains to serve $K = Q$ UEs. Differing from [2], [8], the BS is assumed to be equipped with both phase-shifters (PS) and switches, as shown in Fig. 1. The BS antennas are grouped into Q sub-arrays. Antennas in each sub-array are associated with one particular RF chain. Using this hybrid architecture with both switches and PSs, the BS can adopt two working modes: 1) partial-connected PS network (as A2 in [8]), hereafter referred to as PS mode; 2) partially-connected switch network (as A6 in [8]), hereafter referred to as SW mode. In PS mode, each RF chain can connect to N/Q antennas via PSs. In SW mode, each RF chain can connect to one antenna in its sub-array. When working in SW mode, the BS has a fully digital architecture with dimension Q . For the BS, the implementation of a switch network enables the access to the received signal from an individual antenna, which is useful for channel estimation, especially when SNR

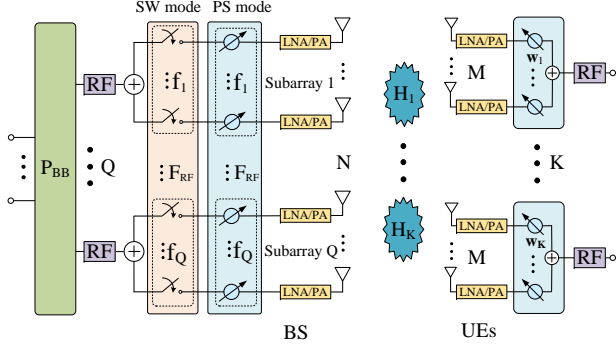


Fig. 1. System architectures for BS and UE, the RF part of BS has two modes of operation: 1) phase-shifter-based mode (PS mode) for directional data transmission and 2) switch-based mode (SW mode) for channel estimation.

is high. In contrast, the PS network is used to perform analog beamforming and combining for both beam training and data transmission.

Compared to BS, each UE has M antennas and only one RF chain. It can use M PSs to perform beam steering. This UE architecture has low complexity and low energy consumption which is suitable for mobile devices. With such a UE architecture, a UE using one specific RF codeword can be treated as a single-antenna device with a specific beam pattern, from the perspective of BS.

The BS has two kinds of RF precoder/combiner depending on the working modes. In SW mode, the sub-array RF precoder/combiner \mathbf{f}_q is an antenna selection vector with one non-zero element. In PS mode, \mathbf{f}_q is a sub-array steering vector. For UEs, the RF precoder/combiner \mathbf{w}_k of UE k is a beam steering vector. We assume that BS and UE have Q_{ps} -bits quantized PSs [15]. The number of beams that can be steered by BS or UE depends on the PS resolution Q_{ps} rather than the number of antennas and is equal to $2^{Q_{\text{ps}}}$. The coefficient set available for each PS is denoted by $\mathbb{P} = \{\omega^0, \omega^1, \dots, \omega^{2^{Q_{\text{ps}}}-1}\}$ with $\omega = e^{j2\pi/2^{Q_{\text{ps}}}}$ as the minimum angular domain separation. The quantized PSs can only adjust the phases of the signals. Thus the elements of the phased precoders and combiners should have constant modulus constraints. More specifically, we have

$$\mathbf{f}_q = \mathbf{1}_{\Omega_q} \odot \mathbf{f}_\omega(c, N), \quad \mathbf{w}_k = \mathbf{f}_\omega(c, M), \quad (1)$$

where Ω_q is the antenna index set for q th sub-array, $\mathbf{1}_{\Omega_q}$ is a binary valued vector with $|\Omega_q|$ ones indexed by Ω_q , $\mathbf{f}_\omega(c, i) = [1, \omega^c, \omega^{2c}, \dots, \omega^{(i-1)c}]^T$ and $c \in \{0, 1, \dots, 2^{Q_{\text{ps}}}-1\}$.

B. Channel Model

MmWave channels are highly directional and sparse in the angular domain [16]. Due to the extremely short wave-length, diffraction in mmWave frequencies is small, so that only line-of-sight (LoS) and reflected paths are significant. This makes that the number of paths quite smaller than the dimensions of BS arrays. Suppressing the vertical directivity of the channel, for the k th UE, the DL channel is then modeled as [2],

$$\mathbf{H}_k = \sum_{l=1}^L \alpha_l \mathbf{a}_{\text{UE}}(\theta_l) \mathbf{a}_{\text{BS}}(\phi_l)^H \in \mathbb{C}^{M \times N}, \quad (2)$$

where L represents the number of paths, and α_l denotes the complex gain of the l th path. In addition, $\mathbf{a}_{\text{BS}}(\phi_l)$ and

$\mathbf{a}_{\text{UE}}(\theta_l)$ represent the BS and UE array response vectors for the l th path, where ϕ_l is the DOD at BS, and θ_l is DOA at UE. Considering plane-wave model and uniform linear array (ULA) for both BS and UE, the array steering vectors can be written as

$$\begin{aligned} \mathbf{a}_{\text{BS}}(\phi) &= [1, e^{j\frac{2\pi}{\lambda}d\sin(\phi)}, \dots, e^{j(N-1)\frac{2\pi}{\lambda}d\sin(\phi)}]^T, \\ \mathbf{a}_{\text{UE}}(\theta) &= [1, e^{j\frac{2\pi}{\lambda}d\sin(\theta)}, \dots, e^{j(M-1)\frac{2\pi}{\lambda}d\sin(\theta)}]^T, \end{aligned} \quad (3)$$

where λ is carrier wavelength and antenna spacing here is assumed to be $d = \lambda/2$. We assume that the system is working in the time division duplex (TDD) mode, and that DL/UL channels are symmetric according to the channel reciprocity by ignoring possible calibration errors. As a result, the UL channel for UE k is \mathbf{H}_k^H .

Assuming $\mathbf{P}_{\text{BB}} = [\mathbf{p}_1, \dots, \mathbf{p}_K] \in \mathbb{C}^{Q \times K}$ is the BS baseband MU combiner or precoder, $\mathbf{F}_{\text{RF}} = [\mathbf{f}_1, \dots, \mathbf{f}_Q] \in \mathbb{C}^{N \times Q}$ is the BS RF combiner or precoder, $\mathbf{W} = [\mathbf{w}_1, \dots, \mathbf{w}_K] \in \mathbb{C}^{M \times K}$ is the RF combiner or precoder for all K UEs. The DL and the UL received signals including interference and noise for the k th UE are

$$\begin{aligned} z_u &= \mathbf{w}_k^H \mathbf{H}_k \mathbf{F}_{\text{RF}} (\mathbf{p}_k x_k + \sum_{j \neq k} \mathbf{p}_j x_j) + \mathbf{w}_k^H \mathbf{n}_u, \\ z_b &= \mathbf{p}_k^H \mathbf{F}_{\text{RF}}^H (\mathbf{H}_k^H \mathbf{w}_k y_k + \sum_{j \neq k} \mathbf{H}_j^H \mathbf{w}_j y_j + \mathbf{n}_b), \end{aligned} \quad (4)$$

where x_k and y_k are the DL and UL signals, satisfying $\mathbb{E}(x_k x_k^*) = \frac{\rho_{\text{BS}}}{K}$ and $\mathbb{E}(y_k y_k^*) = \frac{\rho_{\text{UE}}}{M}$ with transmit powers as ρ_{BS} and ρ_{UE} . In addition, $\mathbf{n}_u \in \mathbb{C}^{M \times 1}$ is the $\mathcal{CN}(0, \sigma_u^2)$ UE noise vector with noise power σ_u^2 per antenna, and $\mathbf{n}_b \in \mathbb{C}^{N \times 1}$ is the $\mathcal{CN}(0, \sigma_b^2)$ BS noise vector with noise power σ_b^2 per antenna. For DL transmission, $\mathbf{F} = \mathbf{F}_{\text{RF}} \mathbf{P}_{\text{BB}}$ satisfies power constraint $\text{tr}(\mathbf{F}\mathbf{F}^H) \leq 1$. For UL transmission, \mathbf{w}_k satisfies $\|\mathbf{w}_k\|_2^2 \leq M$.

III. PROBLEM FORMULATION FOR CHANNEL ESTIMATION

For channel training in UL, we assume that the k th UE will transmit the pilot sequence $\mathbf{s}_k \in \mathbb{C}^{T_s \times 1}$ using beam codeword \mathbf{w}_k . Assuming $\mathbf{P}_{\text{BB}} = \mathbf{I}_Q$, the received training signal at BS is

$$\mathbf{Y} = \mathbf{F}_{\text{RF}}^H (\sum_{k=1}^K \mathbf{h}_k \mathbf{s}_k^T + \mathbf{N}_b) \quad (5)$$

where $\mathbf{h}_k = \mathbf{H}_k^H \mathbf{w}_k$ is the effective user channel when UE k uses beam codeword \mathbf{w}_k . The user pilots are assumed to satisfy $\mathbf{s}_k^H \mathbf{s}_{k'} = \frac{T_s \rho_{\text{UE}}}{M} \delta_{k, k'}$. Correlating \mathbf{Y} with \mathbf{s}_k for the k th UE, we get

$$\mathbf{y}_k = \mathbf{Y} \mathbf{s}_k^* = \sqrt{T_s \rho_{\text{UE}}} \mathbf{F}_{\text{RF}}^H \mathbf{h}_k + \mathbf{F}_{\text{RF}}^H \mathbf{N}_b \mathbf{s}_k^*. \quad (6)$$

Assuming the BS performs T snapshots of measurements with different precoding matrices \mathbf{F} , and stacking the $W = T \times Q$ measurement results, we have

$$\mathbf{z} = \begin{bmatrix} \mathbf{y}_{1,k} \\ \mathbf{y}_{2,k} \\ \vdots \\ \mathbf{y}_{T,k} \end{bmatrix} = \underbrace{\sqrt{T_s \rho_{\text{UE}}} \begin{bmatrix} \mathbf{F}_{1,\text{RF}}^H \\ \mathbf{F}_{2,\text{RF}}^H \\ \vdots \\ \mathbf{F}_{T,\text{RF}}^H \end{bmatrix}}_{\Phi} \mathbf{h}_k + \underbrace{\begin{bmatrix} \mathbf{F}_{1,\text{RF}}^H \mathbf{N}_{1,b} \\ \mathbf{F}_{2,\text{RF}}^H \mathbf{N}_{2,b} \\ \vdots \\ \mathbf{F}_{T,\text{RF}}^H \mathbf{N}_{T,b} \end{bmatrix}}_{\mathbf{n}} \mathbf{s}_k^*, \quad (7)$$

where Φ is the sensing matrix, \mathbf{z} is the measurement and \mathbf{n} is the noise after combining. The objective of UL channel

estimation is to estimate the effective channel from the UE pilots. From (2), we have

$$\mathbf{h}_k = \mathbf{H}_k^H \mathbf{w}_k = \sum_{l=1}^L \beta_l \mathbf{a}_{\text{BS}}(\phi_l), \quad (8)$$

where $\beta_l = (\alpha_l (\mathbf{w}_k)^H \mathbf{a}_{\text{UE}}(\theta_l))^*$. The effective channel \mathbf{h}_k is sparse in the angular domain, and we can use CS-based methods to estimate it. To estimate \mathbf{h}_k , one just need to estimate DOAs $\{\phi_l\}$ and the complex gains $\{\beta_l\}$ for those L paths. In grid-based CS methods, a discrete dictionary $\Psi_{\text{BS}} = [\mathbf{a}_{\text{BS}}(\phi_1), \dots, \mathbf{a}_{\text{BS}}(\phi_{G_b})]$ with G_b bases is used to represent the channel \mathbf{h}_k . More specifically, we have

$$\mathbf{h}_k = \Psi_{\text{BS}} \mathbf{h}_v, \quad (9)$$

where $\mathbf{h}_v \in \mathbb{C}^{G_b \times 1}$ is the sparse virtual channel in dictionary Ψ_{BS} . Denoting $\mathbf{A} = \Phi \Psi_{\text{BS}}$, to estimate the sparse virtual channel \mathbf{h}_v , one needs to solve the following optimization problem

$$\underset{\mathbf{h}_v}{\text{minimize}} \|\mathbf{h}_v\|_0 \quad \text{s.t.} \quad \|\mathbf{z}_k - \mathbf{A} \mathbf{h}_v\|_2^2 \leq \eta. \quad (10)$$

where η is an optimization parameter and typically set as the noise power after combining. In contrast to [5], we consider the switch-based method for constructing the sensing matrix, in which only Q individual antennas are sampled during one snapshot of measurement. We call this method Antenna Domain Sub-Sampling (ADSS). It is based on SW mode at BS, and the sensing matrix has the following structure,

$$\Phi = \sqrt{T_s \rho_{\text{UE}}} [\mathbf{e}_{i_{1,1}}, \mathbf{e}_{i_{1,2}}, \dots, \mathbf{e}_{i_{1,Q}}, \dots, \mathbf{e}_{i_{T,Q}}]^H, \quad (11)$$

where the unit vector $\mathbf{e}_{i_{t,q}}$ has an element equal to 1 at position $i_{t,q}$, and $i_{t,q}$ ($1 \leq t \leq T, 1 \leq q \leq Q$) is the antenna index for the q th RF chain in the t th measurement snapshot. Furthermore, if we define the antenna index set $\Omega = \{i_{1,1}, i_{1,2}, \dots, i_{1,Q}, \dots, i_{T,Q}\}$ for all sampled antennas, we have

$$\mathbf{z} = \Phi \mathbf{h}_k + \mathbf{n} = \sqrt{T_s \rho_{\text{UE}}} (\mathbf{h}_k)_\Omega + \mathbf{n}. \quad (12)$$

A variety of algorithms have been proposed for obtaining an approximate solution to (10) at polynomial complexity, and OMP is a preferred method due to its simplicity and fast implementation [5]. To solve (10) based on the measurement data \mathbf{z} in (12), we use OMP as in Algorithm 1. The computational complexity of OMP is proportional to the number G_b of grid points. Step 3 in Algorithm 1 needs $\mathcal{O}(W G_b)$ computations and solving the least square (LS) problem in step 5 requires $\mathcal{O}(W |\mathcal{I}_t|^2)$.

The joint design of the sensing matrix Φ and the dictionary matrix Ψ plays a key role in the successful reconstruction of the channel \mathbf{h}_k . The mutual coherence of a dictionary matrix \mathbf{A} is $\mu(\mathbf{A}) = \max |\mathbf{a}_i^H \mathbf{a}_j|$, which is the largest inner product of two normalized columns in \mathbf{A} . To reconstruct \mathbf{h}_v (hence \mathbf{h}_k), \mathbf{A} should have low mutual coherence. More specifically, one can guarantee that MP algorithms can reconstruct \mathbf{h}_k successfully [8] in the noiseless case if

$$\mu(\mathbf{A}) < \frac{1}{2\hat{L} - 1}, \quad (13)$$

where \hat{L} is the sparsity, i.e., the number of the nonzero elements in \mathbf{h}_v . A lower bound of $\mu(\mathbf{A})$ is given by the Welch

Algorithm 1 OMP for effective channel estimation

Input: The sensing matrix Φ , the dictionary matrix Ψ_{BS} and $\mathbf{A} = \Phi \Psi_{\text{BS}} = [\mathbf{a}_1, \mathbf{a}_2, \dots, \mathbf{a}_{G_b}]$, the measurement vector \mathbf{z} , and a threshold δ .

- 1: Iteration counter $t \leftarrow 0$, basis vector set $\mathcal{I}_t \leftarrow \emptyset$, virtual channel $\mathbf{h}_v \leftarrow \mathbf{0} \in \mathbb{C}^{G_b \times 1}$, residual error $\mathbf{r}_t \leftarrow \mathbf{z}$
- 2: **while** $\|\mathbf{r}\| > \delta$ and $t < G_b$ **do**
- 3: $g^* \leftarrow \arg \max_g \|\mathbf{a}_g^H \mathbf{r}_t\|_2$ \triangleright Find new basis vector
- 4: $t \leftarrow t + 1$, $\mathcal{I}_t \leftarrow \mathcal{I}_{t-1} \cup \{g^*\}$ \triangleright Update vector set
- 5: $\mathbf{x}^* \leftarrow \arg \min_{\mathbf{x}} \|\mathbf{z} - (\mathbf{A})_{\mathcal{I}_t} \mathbf{x}\|_2$ \triangleright LS method
- 6: $\mathbf{r}_t \leftarrow \mathbf{z} - (\mathbf{A})_{\mathcal{I}_t} \mathbf{x}^*$ \triangleright Update residual error
- 7: $(\mathbf{h}_v)_{\mathcal{I}_t} \leftarrow \mathbf{x}^*$ \triangleright Update the virtual channel
- 8: **end while**

Output: Estimated channel $\hat{\mathbf{h}} = \Psi_{\text{BS}} \mathbf{h}_v$

bound [8] as $\mu(\mathbf{A}) \geq \sqrt{\frac{G_b - W}{W(G_b - 1)}}$, with \mathbf{A} of size $W \times G_b$. This lower bound decreases as the number of measurements W increases.

IV. ATOMIC NORM MINIMIZATION FOR EQUIVALENT CHANNEL ESTIMATION

When using the dictionary Ψ_{BS} for channel estimation via OMP, the estimated path angles are considered to be on a discrete grid $\{\phi_1, \dots, \phi_{G_b}\}$, which introduces the basis mismatch problem [7]. To avoid this, we consider a continuous dictionary for estimating the effective channel.

To estimate the effective channel based on UL measurements, the following constrained optimization problem can be solved:

$$\underset{\mathbf{h}}{\text{minimize}} \mathcal{M}(\mathbf{h}) \quad \text{s.t.} \quad \|\mathbf{z} - \Phi \mathbf{h}\|_2^2 \leq \eta. \quad (14)$$

Here $\mathcal{M}(\mathbf{h})$ denotes a sparse metric to be minimized for a channel vector \mathbf{h} . The noise is assumed to be bounded by $\|\mathbf{n}\|_2^2 \leq \eta$, and \mathbf{h} can be treated as the signal of interest which needs to be estimated based on the observed data \mathbf{z} in the context of line spectral estimation [12]. Problem (14) differs from (10) as it is formulated without a discrete dictionary. Instead of (14), one can solve a regularized optimization problem

$$\underset{\mathbf{h}}{\text{minimize}} \xi \mathcal{M}(\mathbf{h}) + \frac{1}{2} \|\mathbf{z} - \Phi \mathbf{h}\|_2^2, \quad (15)$$

where $\xi > 0$ is a regularization parameter related to η . There are different choices for $\mathcal{M}(\mathbf{h})$ [7]. Here, we consider the atomic norm $\mathcal{M}(\mathbf{h}) = \|\mathbf{h}\|_{\mathcal{A}}$ proposed in [7]. The atomic norm has been widely used in grid-less compressive sensing for a range of applications [7], [12]–[14], including DOA estimation, line spectral estimation and massive MIMO channel estimation. The continuous set of atoms used to represent \mathbf{h} is defined as:

$$\mathcal{A} = \left\{ \mathbf{a}_{\text{BS}}(\phi) \alpha : \phi \in \left(-\frac{\pi}{2}, \frac{\pi}{2}\right], \alpha \in \mathbb{C}, |\alpha| = 1 \right\}. \quad (16)$$

The atomic norm is the gauge function [17] of the convex hull $\text{conv}(\mathcal{A})$. Formally, the atomic norm can be written as

$$\begin{aligned} \|\mathbf{h}\|_{\mathcal{A}} &= \inf \{g > 0 : \mathbf{h} \in g \cdot \text{conv}(\mathcal{A})\} \\ &= \inf \left\{ \sum_i b_i : \mathbf{h} = \sum_i b_i \mathbf{a}_i, b_i > 0, \mathbf{a}_i \in \mathcal{A} \right\}. \end{aligned} \quad (17)$$

The atomic norm is a continuous counterpart of the ℓ_1 -norm used in on-grid CS methods. It can be computed efficiently via semidefinite programming [7]. Specifically, $\|\mathbf{h}\|_{\mathcal{A}}$ defined in (17) is the optimal value of the following matrix trace minimization problem:

$$\underset{\mathbf{u}, t}{\text{minimize}} \quad \frac{1}{2}(t + u_1) \quad \text{s.t.} \quad \begin{bmatrix} \mathcal{T}(\mathbf{u}) & \mathbf{h} \\ \mathbf{h}^H & t \end{bmatrix} \succeq \mathbf{0}, \quad (18)$$

where $\mathcal{T}(\mathbf{u})$ is a Hermitian Toeplitz matrix with its first row as $\mathbf{u} = [u_1, \dots, u_N]^T$. In the noisy case, using the atomic norm, we can rewrite the optimization problem (15) as

$$\underset{\mathbf{D} \succeq \mathbf{0}}{\text{minimize}} \quad \frac{\xi}{2}(t + u_1) + \frac{1}{2} \|\mathbf{z} - \Phi \mathbf{h}\|_2^2 \quad (19)$$

$$\text{s.t.} \quad \mathbf{D} = \begin{bmatrix} \mathcal{T}(\mathbf{u}) & \mathbf{h} \\ \mathbf{h}^H & t \end{bmatrix}.$$

The above problem is a SDP which can be solved by off-the-shelf convex optimization tools in polynomial time [18], and the computational complexity is $\mathcal{O}((N+1)^6)$ in each iteration using the interior point method.

To guarantee that \mathbf{h} can be exactly recovered by ANM, the antenna sampling index set Ω and the number of spatial frequencies in \mathbf{h} (i.e. the number of paths L in the user channel) should satisfy a condition which is similar to the mutual coherence condition used in grid-based CS. To define this condition for ANM, we need the concept called spark for the continuous set of atoms. Let us define the continuous dictionary with sampling index set Ω as

$$\mathbf{A}_\Omega = \{\mathbf{a}_\Omega(f) = (\mathbf{a}(f))_\Omega : f \in \mathbb{F}\}. \quad (20)$$

In the discrete case, the spark of a matrix \mathbf{A} is the smallest number s such that there exists a set of s columns in \mathbf{A} which are linearly dependent. Similar to the definition of matrix spark, the spark of \mathbf{A}_Ω is defined as the smallest number of atoms which are linearly dependent in \mathbf{A}_Ω , denoted by $\text{spark}(\mathbf{A}_\Omega)$. From [17], we have that the problem (14) with $\eta = 0$ in the noiseless setting has a unique solution $\mathbf{h} = \sum_{i=1}^L c_i \mathbf{a}(f_i, \alpha_i)$ if the number of paths satisfies

$$L < \frac{\text{spark}(\mathbf{A}_\Omega)}{2}. \quad (21)$$

Note that the spark of \mathbf{A} in (13) satisfies $\text{spark}(\mathbf{A}) \geq 1 + (\mu(\mathbf{A}))^{-1}$, so that the condition above is equivalent to (13) in the case of discrete atoms. The $\text{spark}(\mathbf{A}_\Omega)$ should be as large as possible so that ANM can recover a channel with more paths. The calculation of a matrix spark is a NP-hard problem, and so it is for the continuous dictionary. One may notice that $\text{spark}(\mathbf{A}_\Omega)$ depends only on Ω , including the size $|\Omega|$ and the sampled antenna indexes. It was shown that $2 \leq \text{spark}(\mathbf{A}_\Omega) \leq |\Omega| + 1$, and a random Ω or a Ω with $|\Omega|$ consecutive integers can achieve a sufficiently large spark [17].

In this section, we have turned to the atomic norm approach for the estimation of the sparse effective user channel \mathbf{h}_k , and have shown that the estimation problem can be cast as SDP and be solved in polynomial time. We will evaluate performance of both OMP and ANM in section VI.

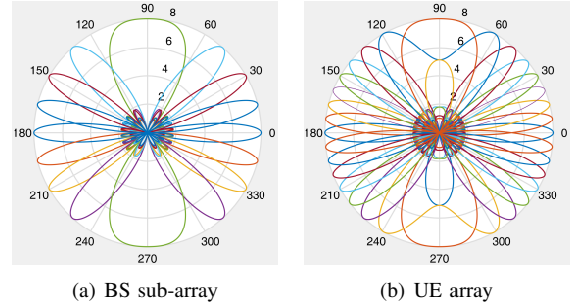


Fig. 2. (a) Designed Q DL sub-array beams with $N = 64, Q = 8, Q_{\text{ps}} = 4$; (b) Designed 16 UE beams with $M = 8, Q_{\text{ps}} = 4$.

V. MU DOWNLINK PRECODING/COMBINING BASED ON THE ESTIMATED CHANNELS

In this section, we consider the designs of downlink BS precoder and UE combiners. To design the BS precoder $\{\mathbf{F}_{\text{RF}}, \mathbf{P}_{\text{BB}}\}$ and UE combiners \mathbf{W} optimally, full CSI $\mathcal{H} = \{\mathbf{H}_1, \mathbf{H}_2, \dots, \mathbf{H}_K\}$ needs to be known. However, acquiring \mathcal{H} would require each UE to send huge amount of pilots which consumes lots of resources. A sub-optimal method, which works well when user channels are sparse, is that UEs first find their best beams independently which aligns with their most significant path. We consider a simple UE beam training scheme first, and then UEs transmit their pilots to BS for MU channel estimation as discussed in sections III and IV. As a result, the BS only needs to estimate the user effective channel \mathbf{h}_k . BS will then design the its MU precoder based on those estimated effective channels. For UEs, the beam codebook is

$$\mathcal{U} = \{\mathbf{f}_\omega(c, M) : c \in \{0, \dots, 2^{Q_{\text{ps}}} - 1\}\}. \quad (22)$$

For BS, the DL training beam codebook used by the q th sub-array is

$$\mathcal{F}_q = \{\mathbf{1}_{\Omega_q} \odot \mathbf{f}_\omega(c, N) : c \in \{0, \dots, 2^{Q_{\text{ps}}} - 1\}\}. \quad (23)$$

Sub-array q will use one beam from \mathcal{F}_q for UE beam training. Fig. 2 (a) shows the designed DL beams used for the BS sub-arrays and Fig. 2 (b) shows the UE beam codebook we used.

The objective of the UE beam training is to find a UE beam which maximizes the norm of the effective channel

$$\underset{\mathbf{w}_k \in \mathcal{U}}{\text{maximize}} \quad \|\mathbf{w}_k^H \mathbf{H}_k\|_2^2, \quad (24)$$

The problem in (24) is equivalent to finding the best steering vector $\mathbf{w}_k \in \mathcal{U}$ that aligns with those paths which have large path gains. In principle, to find the best UE codeword, BS needs to transmit DL training beams which cover all the paths. However, this would increase the training overhead. We propose using all sub-arrays to transmit Q DL pilots with Q sub-array beams simultaneously which are evenly distributed in $[-\pi/2, \pi/2)$. The MU precoding scheme based on UE beam training and effective channel estimation is summarised and shown in Algorithm 2.

VI. NUMERICAL RESULTS

In this section, we will evaluate the performance of the proposed channel estimation method and the precoding scheme via numerical simulations. We assume $M = 8$ for UEs, and

Algorithm 2 Joint UE combining and BS MU precoding

- 1: BS transmits Q DL pilots using Q sub-arrays
 - 2: Each UE $k \in \{1, 2, \dots, K\}$ receives DL pilots using codewords from UE codebook $\mathcal{U} = \{\mathbf{w}^{(1)}, \dots, \mathbf{w}^{(P)}\}$ and calculate the received power with the p th UE beam and q th BS DL beam, each UE then has a received power matrix $\mathbf{P}_k = [\mathbf{p}_1, \mathbf{p}_2, \dots, \mathbf{p}_Q] \in \mathbb{R}^{|\mathcal{U}| \times Q}$. Let $\mathbf{c} \leftarrow \mathbf{0}_{|\mathcal{U}| \times 1}$,
 - 3: **for** $q = 1, 2, \dots, Q$ **do**
 - 4: Find the best UE beam i^* for the q th BS beam:
 - 5: $i^* \leftarrow \operatorname{argmax}_i (\mathbf{p}_q)_i$, $(\mathbf{c})_{i^*} \leftarrow (\mathbf{c})_{i^*} + (\mathbf{p}_q)_{i^*}$.
 - 6: Find the final best UE beam:
 - 7: $p^* \leftarrow \operatorname{argmax}_i (\mathbf{c})_i$, $\mathbf{w}_k \leftarrow \mathbf{w}^{(p^*)}$
 - 8: **end for**
 - 9: UE k transmits UL pilot to BS using \mathbf{w}_k , the BS estimates the effective user channel \mathbf{h}_k using OMP or ANM methods as described in sections III and IV. the BS has an estimated MU channel $\hat{\mathbf{H}} = [\hat{\mathbf{h}}_1, \hat{\mathbf{h}}_2, \dots, \hat{\mathbf{h}}_K]^H$. Let $\mathbf{F}_{\text{RF}} = [\mathbf{f}_1, \dots, \mathbf{f}_Q] \leftarrow \mathbf{0}_{N \times Q}$,
 - 10: **for** $q \in \{1, 2, \dots, Q\}$ **do**
 - 11: Select UE $k = q$, find $\mathbf{f}_q = \operatorname{argmax}_{\mathbf{f} \in \mathcal{F}_q} |\hat{\mathbf{h}}_k^H \mathbf{f}|^2$
 - 12: **end for**
 - 13: Design \mathbf{P}_{BB} using ZF as $\mathbf{P}_{\text{BB}} = \frac{(\hat{\mathbf{H}}\mathbf{F}_{\text{RF}})^{-1}}{\|\mathbf{F}_{\text{RF}}(\hat{\mathbf{H}}\mathbf{F}_{\text{RF}})^{-1}\|_{\text{F}}}$
-

$N = 64$, $Q = 8$ for BS. The BS antennas are grouped into Q sub-arrays with equal size. We have implemented a channel model in which only reflection and LOS paths are considered. The reflected paths are calculated via ray-tracing and the reflection coefficients are computed based on the Fresnel equation. The relative permittivities of building walls are uniformly distributed between 3 and 7. We consider an outdoor small cell where BS is lower than buildings, and signals will be reflected or blocked by the walls. BS is at the center while UEs are dropped outdoor with distances to BS smaller than 150 meters, as shown in Fig. 3. When calculating path coefficients, up to 3-order reflections are considered. The path coefficient is

$$\alpha_l = e^{j\psi} \sqrt{G_0 x^{-2} g_1(\theta_l) g_2(\phi_l) \prod_{i=0}^R |r_i|^2}, \quad (25)$$

where $G_0 = 10^{-6.14}$ is the omnidirectional path gain [19] at reference distance one meter, x is the path propagation distance in meter, $\psi \sim U(0, 2\pi)$ is the random phase, $g_1(\theta_l)$ and $g_2(\phi_l)$ are UE and BS antenna element patterns respectively, R is the reflection order and r_i is the i th reflection coefficient, with $R = 0$, $r_0 = 1$ for the LOS path. More details of simulation parameters are given in Tab e I.

A. Effective Uer Channel Estimation via OMP and ANM

All UEs transmit orthogonal pilots to BS using their best beams, and BS receives them via ADSS. In these simulations, $T = 2$ measurement snapshots are used, so we have $T \times Q = 16$ antennas sampled pseudo-randomly via the switch network. The estimation error for \mathbf{h}_k is defined as $\|\mathbf{h}_k - \hat{\mathbf{h}}_k\|_2^2 / \|\mathbf{h}_k\|_2^2$. The ANM problem (19) is solved via the SDPT3 [18] solver. Fig. 4 shows the estimation results for two example UEs. The channels are illustrated by the

TABLE I
SIMULATION PARAMETERS

Parameter	Symbol	value
BS hight	h_{BS}	5 m
UE hight	h_{UE}	1.5 m
Carrier frequency	f_c	28 GHz
System bandwidth	b_w	256 MHz
OFDM subcarrier number	N_c	256
UE total Tx power	$N_c \times \rho_{\text{UE}}$	23 dBm
BS total Tx power	$N_c \times \rho_{\text{BS}}$	40 dBm
UE noise power	$N_c \times \sigma_{\text{u}}^2$	-89 dBm
BS noise power	$N_c \times \sigma_{\text{b}}^2$	-86 dBm
UE antenna pattern	$g_1(\theta)$	omnidirectional
BS antenna pattern	$g_2(\phi)$	defined in [20]

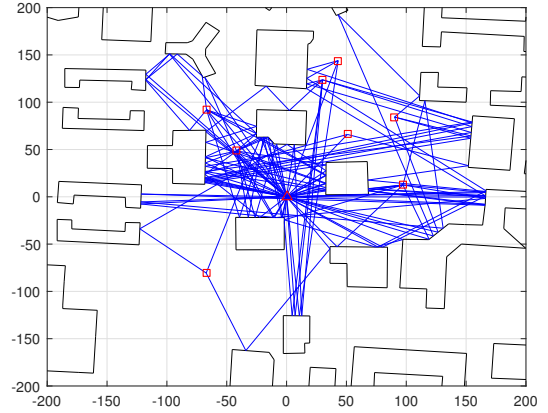


Fig. 3. Simulation scenario in a $400 \times 400 \text{ m}^2$ area, the polygons represent the buildings with walls, red triangle is the BS and red squares are the UEs. Ray-tracing is used to generate the channel paths which are shown in blue lines.

angular domain power $P(\phi) = |\mathbf{h}_k^H \mathbf{a}_{\text{BS}}(\phi)|^2$. Fig. 5 shows the average estimation error for 8000 random UEs with different channel SNRs. As we can see, OMP suffers from basis mismatch. The channel estimation results are inaccurate in high SNR region, producing an error floor. In comparison, ANM achieves much better estimation accuracy, especially in the high SNR regime, effectively removing the error floor. Inaccurate channel estimation degrades the interference

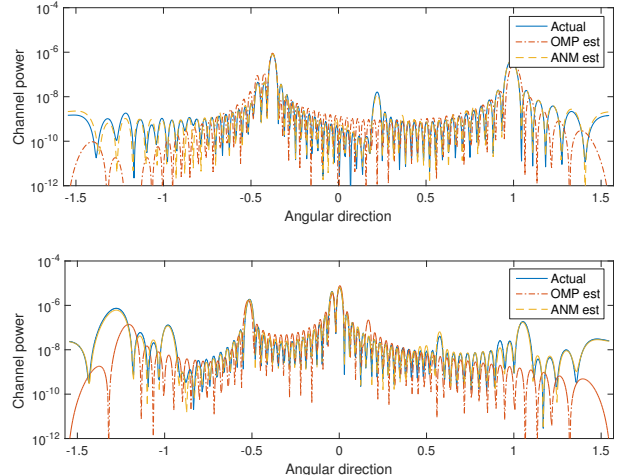


Fig. 4. Example of OMP and ANM estimation results, which show that ANM provides accurate channel estimation while OMP suffers from the mismatch.

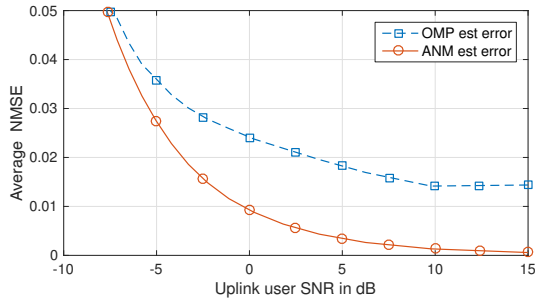


Fig. 5. The average channel estimation error, where the UL SNRs before precoding and combining is $\text{SNR} = \frac{\rho_{\text{UE}} \|\mathbf{H}_k\|_F^2}{MN\sigma_b^2}$.

mitigation performance in MU DL precoding techniques. As a result, ANM would be a strong candidate for the hybrid precoding solution discussed in section V. We also found that in the simulated scenario, the user effective channel \mathbf{h}_k is sparse in angular domain. In most cases, there are one to three significant paths even when the original channel \mathbf{H}_k has much more paths. This ensures that the condition (21) is satisfied and ANM can recover the channel with high probability. In the case that the condition (21) is not satisfied, ANM could recover the strongest paths and moderate channel estimation accuracy is still attainable. Compared to OMP, solving the ANM problem using SDPT3 entails much higher complexity. An efficient solver based on the alternating direction method of multipliers (ADMM) [17] technique could be adopted to solve the ANM SDP problem.

B. Spectral Efficiency Performance of Multi-User Precoding

In this section, MU hybrid precoding is considered. Spectral efficiency performance of ZF precoding based on OMP and ANM channel estimations is shown in Fig. 6. There are $K = 8$ users simultaneously served. The performance of hybrid precoding with perfect CSI is also shown in the figure. The baseband ZF precoding is sensitive to channel estimation error and channel estimation error will destroy the user orthogonality provided by ZF. As shown in Fig. 6, hybrid precoding with ANM-based channel estimation can provide much better performance compared to an OMP-based scheme since it provides very accurate channel estimates for the sparse effective user channel. On average, OMP loses 59% of the spectral efficiency of perfect CSI, whereas ANM loses only 2%, which verify the efficacy of ANM.

VII. CONCLUSION

We have formulated the mmWave channel estimation in a hybrid mmWave system with sub-array as an ANM problem which can be efficiently solved via SDP. Compared to the grid-based CS methods, the proposed ANM approach uses a continuous dictionary with sub-sampling in antenna domain via a dedicated switch network. Simulation results shows that ANM can achieve much better channel estimation accuracy compared to the existing grid-based CS methods, and can help multi-user hybrid precoding on BS to achieve significantly better user spectral efficiency performance.

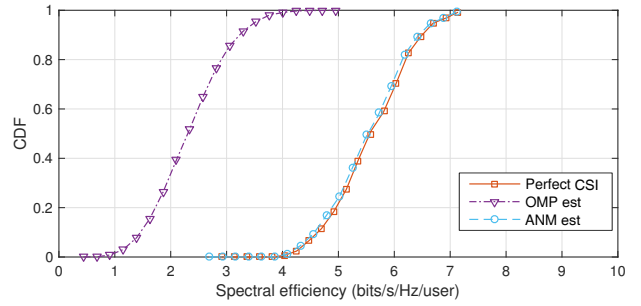


Fig. 6. Performance of low-complexity hybrid precoding with sub-arrays for multiple users with $K = Q = 8$. The number of grid points used for OMP is $G_b = N = 64$.

REFERENCES

- [1] A. Alkhateeb, G. Leus, and R. W. Heath, "Limited feedback hybrid precoding for multi-user millimeter wave systems," *IEEE Trans. Wireless Commun.*, vol. 14, no. 11, pp. 6481–6494, Nov 2015.
- [2] —, "Compressed sensing based multi-user millimeter wave systems: How many measurements are needed?" *Proc. IEEE Int. Conf. Acoustics, Speech and Signal Process. (ICASSP)*, April 2015, pp. 2909–2913.
- [3] Y. Han and J. Lee, "Two-stage compressed sensing for millimeter wave channel estimation," in *Proc. IEEE Int. Symp. Infor. Theory (ISIT)*, July 2016, pp. 860–864.
- [4] A. Alkhateeb et al., "Channel estimation and hybrid precoding for millimeter wave cellular systems," *IEEE J. Sel. Topics Signal Process.*, vol. 8, no. 5, pp. 831–846, Oct 2014.
- [5] J. Lee et al., "Channel estimation via orthogonal matching pursuit for hybrid MIMO systems in millimeter wave communications," *IEEE Trans. Commun.*, vol. 64, no. 6, pp. 2370–2386, June 2016.
- [6] J. Chen and X. Huo, "Theoretical results on sparse representations of multiple-measurement vectors," *IEEE Trans. Signal Process.*, vol. 54, no. 12, pp. 4634–4643, Dec 2006.
- [7] G. Tang et al., "Compressed sensing off the grid," *IEEE Trans. Inf. Theory*, vol. 59, no. 11, pp. 7465–7490, Nov 2013.
- [8] R. Méndez-Rial et al., "Hybrid MIMO architectures for millimeter wave communications: Phase shifters or switches?" *IEEE Access*, vol. 4, pp. 247–267, 2016.
- [9] X. Yu et al., "Alternating minimization algorithms for hybrid precoding in millimeter wave MIMO systems," *IEEE J. Sel. Topics Signal Process.*, vol. 10, no. 3, pp. 485–500, April 2016.
- [10] C. Ekanadham et al., "Recovery of sparse translation-invariant signals with continuous basis pursuit," *IEEE Trans. Signal Process.*, vol. 59, no. 10, pp. 4735–4744, Oct 2011.
- [11] S. Sun and T. S. Rappaport, "Millimeter wave MIMO channel estimation based on adaptive compressed sensing," in *Proc. IEEE Int. Conf. Commun. Workshops (ICCW)*, May 2017, pp. 47–53.
- [12] B. N. Bhaskar et al., "Atomic norm denoising with applications to line spectral estimation," *IEEE Trans. Signal Process.*, vol. 61, no. 23, pp. 5987–5999, Dec 2013.
- [13] P. Zhang et al., "Atomic norm denoising-based channel estimation for massive multiuser MIMO systems," in *Proc. IEEE Int. Conf. Commun. (ICC)*, June 2015, pp. 4564–4569.
- [14] Y. Wang et al., "Efficient channel estimation for massive MIMO systems via truncated two-dimensional atomic norm minimization," in *Proc. IEEE Int. Conf. Commun. (ICC)*, May 2017, pp. 1–6.
- [15] F. Sahrabi and W. Yu, "Hybrid digital and analog beamforming design for large-scale antenna arrays," *IEEE J. Sel. Topics Signal Process.*, vol. 10, no. 3, pp. 501–513, April 2016.
- [16] T. S. Rappaport et al., *Millimeter wave wireless communications*. Pearson Education, 2014.
- [17] Y. Li and Y. Chi, "Off-the-grid line spectrum denoising and estimation with multiple measurement vectors," *IEEE Trans. Signal Process.*, vol. 64, no. 5, pp. 1257–1269, March 1, 2016.
- [18] K.-C. Toh et al., "SDPT3 - A MATLAB software package for semidefinite programming, version 1.3," *Optimization methods and software*, vol. 11, no. 1–4, pp. 545–581, 1999.
- [19] M. R. Akdeniz et al., "Millimeter wave channel modeling and cellular capacity evaluation," *IEEE J. Sel. Areas Commun.*, vol. 32, no. 6, pp. 1164–1179, June 2014.
- [20] 3GPP, "Study on channel model for frequency spectrum above 6 GHz," TR 38.900 V14.3.1, July 2017.